
SEPARATE CHEMICAL FREEZE-OUT OF STRANGE PARTICLES WITH CONSERVATION LAWS
D.R. OLIINYCHENKO,^{1,2} V.V. SAGUN,¹ A.I. IVANYTSKYI,¹ K.A. BUGAEV¹
¹**Bogolyubov Institute for Theoretical Physics, Nat. Acad. of Sci. of Ukraine**
(14b, Metrolohichna Str., Kyiv 03680, Ukraine; e-mail: dimafopf@gmail.com)
²**FIAS, Goethe-University, Frankfurt**
(Ruth-Moufang Str. 1, 60438 Frankfurt upon Main, Germany)

PACS 25.75.-q, 25.75.Nq
©XXXX

The Hadron Resonance Gas Model with two chemical freeze-outs, connected by conservation laws is considered. We are arguing that the chemical freeze-out of strange hadrons should occur earlier than the chemical freeze-out of non-strange hadrons. The hadron multiplicities measured in the heavy ion collisions for the center of mass energy range 2.7 - 200 GeV are described well by such a model. Based on a success of such an approach, a radical way to improve the Hadron Resonance Gas Model performance is suggested. Thus, we suggest to identify the hadronic reactions that freeze-out noticeably earlier or later than most of the others reactions (for different collision energies they may be different) and to consider a separate freeze-out for them.

1. Introduction

The hadronic multiplicities measured in heavy ion collisions and in the collisions of elementary particles are traditionally described by the Hadron Resonance Gas Model (HRGM) [1–5]. It is based on an assumption that the fireballs produced in such collisions reach a full thermal equilibrium. Using this assumption it is possible to describe the hadronic multiplicities registered in experiment with the help of two parameters: temperature T and baryo-chemical potential μ_B . Parameters T and μ_B obtained from the fit of multiplicities for different collision energies correspond to the stage of chemical freeze-out. Its physical meaning is that at this stage the inelastic collisions cease simultaneously for all sorts of particles. However, in such a simple form the concept of chemical freeze-out works well for the hadrons which consists of the u and d (anti)quarks, while the strange hadrons demonstrate deviation from chemical equilibrium.

At the same time the hydrodynamic simulations (see e.g. a review [6]) rather successfully reproduce the transverse momentum spectra of strange particles. This is an old problem of the thermal approach and in order to account for an observed deviation of strange particles from the complete chemical equilibrium the additional parameter γ_s , the strangeness suppression factor, was suggested [7] long ago. Although the concept of strangeness suppression proved to be important both in the collisions of elementary particles [4] and in nucleus-nucleus collisions [4, 8] the problem of its justification remains unsolved. Thus, up to now it is unclear what is the main physical reason which is responsible for chemical non-equilibrium of strange hadrons.

Moreover, it is well known [2] that the fit of hadron multiplicities with the strangeness suppression factor γ_s improves the quality of data description, but still the fit seldom attains a good quality, especially at low collision energies. This is clearly seen from the center of mass energy behavior of two most prominent ratios that involve the lightest strange meson, i.e. K^+/π^+ , and the lightest strange baryon, i.e. Λ/π^- , which, so far, cannot be successfully reproduced [2, 4, 8] by the traditional versions of the HRGM. Also the ratios involving the multi-strange hyperons Ξ and Ω exhibit an apparent failure of the γ_s fit at the center of mass energy $\sqrt{S_{NN}} = 8.76, 12.3$ and 17.3 GeV [2]. Since the γ_s fit does not improve their description sizably, we conclude that there should exist a different reason for the apparent deviation of strange hadrons from chemical equilibrium and, hence, the concept of chemical freeze-out requires a further development.

Recently an alternative concept of chemical freeze-out of strange hadrons was suggested [9]. Instead of a simultaneous chemical freeze-out for all hadrons the two different chemical freeze-outs were suggested: one for particles, containing strange charge, even hidden, (we refer to it as strangeness freeze-out, i.e. SFO) and another one (FO) for all other hadrons which contains only u and d (anti)quarks. A partial justification for the SFO hypothesis is given in [10–12], where the early chemical and kinetic FO of Ω hyperons and J/ψ and ϕ mesons is discussed for the energies at and above the highest SPS energy. In this article we further develop and refine the SFO concept of Ref. [9], and present here a more coherent and detailed picture of two freeze-outs together with new arguments which allow us to better justify and to improve the performance of the HRGM.

The paper is organized as follows. In the next section we discuss the concept of chemical freeze-out in some details and give the arguments that in a meson dominated hadronic medium the SFO should occur earlier than the FO. Section 3 is devoted to a description of the HRGM with the multicomponent hard-core repulsion. The results are presented in Section 4, while Section 5 contains our conclusions and suggestions.

2. The Framework of Thermal Model

In 1950 in his pioneering paper [13] E. Fermi suggested to use the statistical model to find the outcome of high energy nucleon-nucleon collisions. Since in such reactions there were produced from 10 to 30 hadrons, they were named as the processes of multihadron production. According to E. Fermi, the large number of particles in a finale state of these processes naturally suggested to apply the methods of statistical mechanics. The next crucial step suggested by E. Fermi was a justification of the thermal equilibrium assumption due to strong interaction between the particles. A few years later L. D. Landau suggested to apply the relativistic hydrodynamics to the reactions of multihadron production [14], because the applicability conditions of relativistic hydrodynamics are basically the same as for the full (local) thermal equilibrium, if the strong discontinuities are absent.

Since that time an assumption of thermal equilibrium at some stage of the multihadron production reactions was tested experimentally both in the nucleon-nucleon collisions and in the collisions of heavy ions. In other words, the outcome of such reactions was compared to the results of statistical models. A coincidence between the statistical models predictions and the experimental results appeared to be good both for the nucleon-nucleon

collisions and for the heavy ion collisions at energy range starting from the center of mass energy $\sqrt{S_{NN}} = 2$ GeV per nucleon in the fixed target experiments performed at the Brookhaven AGS up to the center of mass energy $\sqrt{S_{NN}} = 2.76$ TeV achieved at the Large Hadron Collider [2, 15]. It was even suggested that for the high energy electron-positron collisions the statistical model can also describe the hadron multiplicities [3]. However, later on a more thorough analysis [16] showed that even within rather sophisticated canonical ensemble consideration the discrepancy between theory and experiment is rather large with $\chi^2/dof > 5$.

Now let us consider in some details a particular set of models used to describe hadron multiplicities in nucleon or heavy ion collisions, that are known as the HRGM [1–5, 8, 15]. A common feature of this set of models is an assumption that at some moment there exists a fireball consisting of all possible hadronic states being locally in thermal and chemical equilibrium. The term chemical equilibrium means that rates of forward and backward reactions are equal, i.e. for any hadron specie the rate of its production is equal to the rate of its destruction. The characteristic time of equilibration varies with collision energy, but one can safely say that it lies within the interval of 0.1-10 fm/c [17–19]. This means that one can safely ignore weak interaction, because its characteristic time is essentially longer. Therefore, the baryon charge B , the strange charge S , the isospin projection I_3 , the charm charge C and the bottom charge are conserved in almost all hadron reactions. Some of the most frequent hadronic reactions read: $\pi\pi \rightarrow \rho \rightarrow \pi\pi$, $\pi K \rightarrow K^* \rightarrow \pi K$, $\pi N \rightarrow \Delta \rightarrow \pi N$. They lead to thermal equilibration, but do not change the number of particles. Another reactions, such as $\pi N \rightarrow N^* \rightarrow \Delta\pi \rightarrow N\pi\pi$, change the number of particles and lead to the chemical equilibration. Was such a system of all hadron states kept in a finite box of volume V , it would inevitably equilibrate both thermally and chemically at $t \rightarrow \infty$. Let us define the characteristic time of equilibration between the species A and B τ_{AB} as an average time when N_0 collisions between A and B occurred. If there are only A and B species in the box then $\tau_{AB} \sim \frac{1}{n_A n_B \sigma_{AB}}$, where σ_{AB} is a cross-section of AB reaction and n_A (n_B) denote the concentration of specie A (B). If one considers a gas of many species in the box out of equilibrium, then the equilibration times will be defined from the system of equations (assuming only the reactions $2 \rightarrow 1$ and $1 \rightarrow$

2):

$$\begin{aligned} \frac{dN_i}{dt} = & \sum_{AB} \frac{N_A N_B v_{AB}^{rel}}{V} \sigma_{AB \rightarrow i} - \sum_A \frac{N_i N_A v_{Ai}^{rel}}{V} \sigma_{Ai \rightarrow B} - \\ & - \sum_{CD} \Gamma_{i \rightarrow CD} N_i, \end{aligned} \quad (1)$$

where N_i , N_A , N_B are the number of hadrons of corresponding kind, σ denotes the corresponding cross-sections and Γ is the decay rate. The first term on the right hand side describes the formation of particles of kind i , the second term stands for the particle destruction of this kind in the $2 \rightarrow 1$ reaction and the third term stands for the decays of this kind of particles. From these equations one can see that the larger production cross-section leads to a faster equilibration, while the larger volume leads to a slower equilibration. One can also see that depending on cross-sections of production and decay and also on volume, equilibration times for different species may be different. These equations are, of course, oversimplified, because they do not include the momentum dependencies. If one introduces such dependencies, then one obtains the system of Boltzmann equations, and, hence, Eq. (1) can be regarded as the system of Boltzmann equations averaged over momenta. However, even these oversimplified equations can help to understand the way how a system approaches an equilibrium. For instance, from Eq. (1) one can see that increasing the box volume n times is equivalent to decreasing all the cross-sections n times. One can also see that for very large volumes only the decays will occur.

If the system is expanding, i.e. $V = V(t)$, then there is no guarantee that all particle species will be at chemical and thermal equilibrium at any time. The simplest way to qualitatively characterize an expanding system is to introduce a set of characteristic times: expansion time t_{ex} , thermalization time t_{th} and chemical equilibration t_{ch} time for different species. It is known that typically for the reactions of strongly interacting particles there is an inequality $t_{ch} \gg t_{th}$ [17–19]. It is equivalent to a statement that cross-sections of reactions which lead to a chemical equilibration are much smaller than the cross-sections of reactions which lead to a thermalization. During the expansion process the system volume increases or equivalently one can say that all cross-sections effectively decrease in the same factor. Therefore, the reactions which lead to a chemical equilibration will cease earlier, than the reactions which lead to a thermalization and they, respectively, are called as chemical and kinetic freeze-out. Since the cross-sections of different reactions are not the same, generally one can

talk about chemical and kinetic freeze-out for each particle specie.

Typically in vacuum the reactions involving strange particles have smaller cross-sections than the reactions involving only non-strange particles (charm and bottom are not considered here at all). Then from our previous consideration one can conclude that, if the cross-sections and the thresholds of hadronic reactions occurring at the late stage of expansion do not differ from their vacuum values, then the chemical equilibrium for strange particles should be lost earlier. The kinetic freeze-out for strange particles is also going to occur earlier than the kinetic freeze-out of non-strange hadrons, but later than the chemical freeze-out for any hadron specie. These conclusions are based on the following hierarchy of the switching off times of hadronic reactions:

$$\begin{aligned} t_{K\Lambda \rightarrow \Sigma p} &> t_{\pi N \rightarrow N^* \rightarrow \Delta \pi \rightarrow N \pi \pi} \gg \\ &\gg t_{K\pi \rightarrow K^* \rightarrow K \pi} > t_{N\pi \rightarrow \Delta \rightarrow N \pi}. \end{aligned} \quad (2)$$

It is not only cross-sections that influence the freeze-out times. As one can see from Eq. (1), the smaller concentrations are, the lower rate of reactions is expected. The numbers of strange particles different from kaons are smaller than the number of protons, and this is one more factor that makes slower the reactions of strangeness exchange and leads to an earlier freeze-outs of strange particles. Of course, one should keep in mind that this simplified treatment is valid at low particle densities, if an approximation of binary reactions is reasonable and if the surrounding medium does not essentially modify the reaction threshold. Therefore, appearing of the results that contradict to the conclusions above should be considered as a signal that the chemical freeze-out picture based on Eqs. (1) and (2) is not justified and, hence, one has to seek for another explanation.

Nevertheless, the argumentation above motivates to consider a separate chemical freeze-out of strange particles in the HRGM. This was done recently in two independent studies [9, 20] and [21]. In [21] three free parameters were taken for FO (temperature, baryon chemical potential and volume) and three free parameters of the same kind for SFO. The electric charge chemical potential μ_Q was taken from the condition $N_B/N_Q = 2.5$ for both freeze-outs. Species subjected to the SFO were all strange particles and the ϕ -mesons. The strange charge was treated canonically and the particle multiplicities were fitted. An approach of [9, 20] is quite different. The parameters of FO and SFO were connected by the conservation laws, namely the baryon number conservation, the I_3 conservation and the entropy conservation. Both freeze-outs were treated grand canonically and the

ϕ mesons were not subjected to earlier freeze-out. Also, in contrast to oversimplified treatment of the equation of state, the HRGM of [9] includes the width of all hadron resonances and the short range repulsion which is taken into account via the excluded volume corrections, while in [21] these important features are neglected.

We would like to stress, although being simple and successful in describing the hadronic multiplicities, an approach suggested in [21] violates the above mentioned conservation laws. Moreover, in such approach it might happen that not only the entropy conservation is violated, but entropy may decrease from an earlier freeze-out to the later one. Finally, while the number of fitted multiplicities is rarely exceeding 10 per one collision energy value, having six fitting parameters for each energy value seems to be excessive. Therefore, below we outline an alternative model [9], which seems to be physically more relevant.

3. Model formulation

In the simplest version the HGRM represents the gas of hadrons being in chemical and thermal equilibrium which is described by the grand canonical partition function. The multiplicity of particles of the mass m_i and degeneracy g_i is given by:

$$N_i = g_i V \int \frac{d^3k}{(2\pi)^3} \frac{1}{e^{\sqrt{m_i^2+k^2}/T-\mu} \pm 1}, \quad (3)$$

where the sign $+(-)$ in the equation above stays for Fermi (Bose) statistics and μ_i denotes the full chemical potential $\mu_i = \mu_B B_i + \mu_S S_i + \mu_{I3} I_{3i}$ of particles of sort i , B_i is their baryonic charge, S_i is their strange charge and I_{3i} denotes their third projection of isospin. The chemical potentials μ_B , μ_S and μ_{I3} which correspond to the conserved charges can be found from the conservation laws

$$\sum_i N_i B_i = B^{init}, \quad (4)$$

$$\sum_i N_i S_i = S^{init}, \quad (5)$$

$$\sum_i N_i I_{3i} = I_3^{init}, \quad (6)$$

then the temperature T and the system volume V will be free parameters. One can, however, take T and μ_B as free parameters and this is a conventional choice. In [22] we argued that for midrapidity the quantities B^{init} and I_3^{init} are anyway unknown, so one can fit the ratios and have T , μ_B and μ_{I3} as the fitting parameters. Using

this procedure one gets the hadron multiplicities that correspond to the full thermal equilibrium. To get the final particle multiplicities, one has to take into account the decays of hadron resonances (see below).

An extension of the HRGM to two freeze-outs is almost obvious in the case of [21], where both non-strange and strange freeze-outs have their own parameters and are by no means connected. In such a case one considers two separate ideal gases with their own parameters. However, if one follows the way described in [9], then some complications arise. One problem is to properly include the conservation laws, then one has to take the excluded volume into account in a consistent way. By consistency we mean that the standard thermodynamic identities should be obeyed. One more issue is the change of entropy between two freeze-outs due to decays of strange resonances. However, as we argued in [9] the latter is negligible, because the time interval between two freeze-outs is short.

Also we would like to stress that the excluded volume for all particles remains the same after the SFO. Indeed, not all reactions between the strange and non-strange particles cease, but only those with the strangeness exchange. For instance, the reaction $\pi K \rightarrow K^* \rightarrow \pi K$ survives after the SFO. It keeps the same excluded volume between pions and kaons, but does not provide the chemical equilibrium for kaons.

After these comments let us formulate our approach. It is based on the multicomponent formulation of the HRGM [5], which is currently the best at describing the observed hadronic multiplicities. Therefore, it is natural to apply such a formulation to describe both the FO and the SFO. The present HRGM was worked out in [5, 22–28]. The interaction between hadrons is taken into account via the hard-core radii, with the different values for pions R_π , kaons R_K , other mesons R_m and baryons R_b . The best fit values for such radii $R_b = 0.2$ fm, $R_m = 0.4$ fm, $R_\pi = 0.1$ fm, $R_K = 0.38$ fm were obtained in [5]. The main equations of the model are listed below, but more details of the model can be found in [5, 22].

We consider the Boltzmann gas of N hadron species in a volume V that has the temperature T , the baryonic chemical potential μ_B , the strange chemical potential μ_S and the chemical potential of the isospin third component μ_{I3} . The system pressure p and the K -th charge density n_i^K ($K \in \{B, S, I3\}$) of the i -th hadron sort are

given by the expressions

$$\frac{p}{T} = \sum_{i=1}^N \xi_i, \quad n_i^K = \frac{Q_i^K \xi_i}{1 + \frac{\xi^T \mathcal{B} \xi}{\sum_{j=1}^N \xi_j}}, \quad \xi = \begin{pmatrix} \xi_1 \\ \xi_2 \\ \dots \\ \xi_N \end{pmatrix}, \quad (7)$$

where \mathcal{B} denotes a symmetric matrix of the second virial coefficients with the elements $b_{ij} = \frac{2\pi}{3}(R_i + R_j)^3$ and the variables ξ_i are the solutions of the following system

$$\xi_i = \phi_i(T) \exp \left[\frac{\mu_i}{T} - \sum_{j=1}^N 2\xi_j b_{ij} + \xi^T \mathcal{B} \xi \left[\sum_{j=1}^N \xi_j \right]^{-1} \right], \quad (8)$$

$$\phi_i(T) = \frac{g_i}{(2\pi)^3} \int \exp \left(-\frac{\sqrt{k^2 + m_i^2}}{T} \right) d^3k. \quad (9)$$

Here the full chemical potential of the i -th hadron sort is defined as before, $\phi_i(T)$ denotes the thermal particle density of the i -th hadron sort of mass m_i and degeneracy g_i , and ξ^T denotes the row of variables ξ_i .

The width correction is taken into account by averaging all expressions containing resonance mass by the Breit-Wigner distribution having a threshold (see, for instance [1], for more details). The effect of resonance decay $Y \rightarrow X$ with the branching ratio $BR(Y \rightarrow X)$ on the final hadronic multiplicity is taken into account as $n^{fin}(X) = \sum_Y BR(Y \rightarrow X) n^{th}(Y)$, where $BR(X \rightarrow X) = 1$ for the sake of convenience. The masses, the widths and the strong decay branchings of all hadrons were taken from the particle tables used by the thermodynamic code THERMUS [29].

The SFO is assumed to occur for all strange particles at the temperature T_{SFO} , the baryonic chemical potential μ_{BSFO} , the isospin third projection chemical potential μ_{ISFO} and the three dimensional space-time extent (effective volume) of the freeze-out hypersurface V_{SFO} . The FO of hadrons which are built of the u and d (anti)quarks, is assumed to be described by its own parameters T_{FO} , μ_{BFO} , μ_{ISFO} , V_{FO} . Eqs. (7)–(9) for FO and SFO remain the same as for a simultaneous FO of all particles. In both cases μ_S is found from the net zero strangeness condition. The major difference of the SFO approach is the presence of conservation laws and the corresponding modification of multiplicities due to resonance decays. Thus, we assume that between two freeze-outs the system is sufficiently dilute and hence its evolution is governed by the continuous hydrodynamic evolution which conserves the entropy. Then equations for the entropy, the baryon charge and the isospin projection conservation connecting two freeze-outs are as

follows:

$$s_{FO} V_{FO} = s_{SFO} V_{SFO}, \quad (10)$$

$$n_{FO}^B V_{FO} = n_{SFO}^B V_{SFO}, \quad (11)$$

$$n_{FO}^{I_3} V_{FO} = n_{SFO}^{I_3} V_{SFO}. \quad (12)$$

Getting rid of the effective volumes we obtain

$$\frac{s}{n^B} \Big|_{FO} = \frac{s}{n^B} \Big|_{SFO}, \quad \frac{n^B}{n^{I_3}} \Big|_{FO} = \frac{n^B}{n^{I_3}} \Big|_{SFO}. \quad (13)$$

Therefore, the variables μ_{BSFO} and μ_{ISFO} are not free parameters, since they are found from the system (13) and only T_{SFO} should be fitted. Thus, for the SFO the number of independent fitting parameters is 4 for each value of collision energy.

The number of resonances appeared due to decays are found from

$$\frac{N^{fin}(X)}{V_{FO}} = \sum_{Y \in FO} BR(Y \rightarrow X) n^{th}(Y) + \sum_{Y \in SFO} BR(Y \rightarrow X) n^{th}(Y) \frac{V_{SFO}}{V_{FO}}. \quad (14)$$

Technically this is done by multiplying all the thermal concentrations for SFO by $n_{FO}^B/n_{SFO}^B = V_{SFO}/V_{FO}$ and applying the conventional resonance decays.

4. Results

Data sets and fit procedure. In our choice of the data sets we basically followed Ref. [2]. Thus, at the AGS energy range of collisions ($\sqrt{S_{NN}} = 2.7 - 4.9$ GeV) the data are available for the kinetic beam energies from 2 to 10.7 AGeV. For the beam energies 2, 4, 6 and 8 AGeV there are only a few data points available: the yields for pions [30, 31], for protons [32, 33], for kaons [31] (except for 2 AGeV), for Λ hyperons the integrated over 4π data are available [34]. For the beam energy 6 AGeV there exist the Ξ^- hyperon data integrated over 4π geometry [35]. However, the data for the Λ and Ξ^- hyperons have to be corrected [2], and instead of the raw experimental data we used their corrected values of Ref. [2]. For the highest AGS center of mass energy $\sqrt{S_{NN}} = 4.9$ GeV (or the beam energy 10.7 AGeV) in addition to the mentioned data for pions, (anti)protons and kaons there exist data for ϕ meson [36], for Λ hyperon [37] and for $\bar{\Lambda}$ hyperon [38]. Similarly to [5], here we analyzed only the NA49 mid-rapidity data [39–44] since they are traditionally the most difficult to describe. Because the RHIC high energy data of different collaborations agree with each other, we present the analysis of the STAR

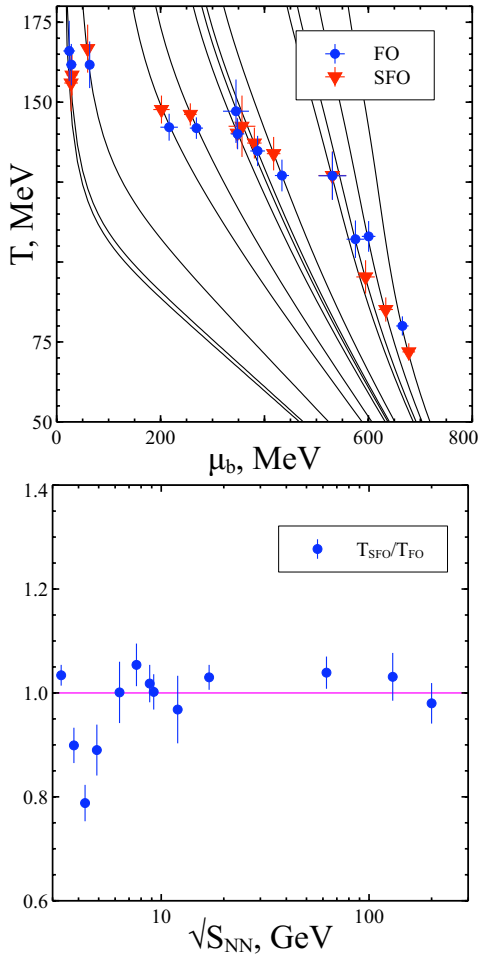


Fig. 1. Parameters of chemical freeze-outs in the model with two freeze-outs. Upper panel: triangles correspond to the SFO, their coordinates are (μ_{BSFO}, T_{SFO}) , while circles correspond to the FO and their coordinates are (μ_{BFO}, T_{FO}) . The curves correspond to isentropic trajectories $s/\rho_B = const$ connecting two freeze-outs. Lower panel: $\sqrt{S_{NN}}$ dependence of the ratio of the SFO temperature to the FO temperature.

results for $\sqrt{S_{NN}} = 9.2$ GeV [45], $\sqrt{S_{NN}} = 62.4$ GeV [46], $\sqrt{S_{NN}} = 130$ GeV [47–50] and 200 GeV [50–52].

To avoid possible biases we fit the particle ratios rather than the multiplicities. The best fit criterion is a minimality of $\chi^2 = \sum_i \frac{(r_i^{theor} - r_i^{exp})^2}{\sigma_i^2}$, where r_i^{exp} is an experimental value of i -th particle ratio, r_i^{theor} is our prediction and σ_i is a total error of experimental value.

Fit results. The FO and the SFO parameters are connected by conservation laws (13). Therefore, for the SFO there is only one fitting parameter at each collision energy, namely T_{SFO} , while other parameters are found from the system (13). We study two things: behavior of parameters and what ratios are improved in the SFO ap-

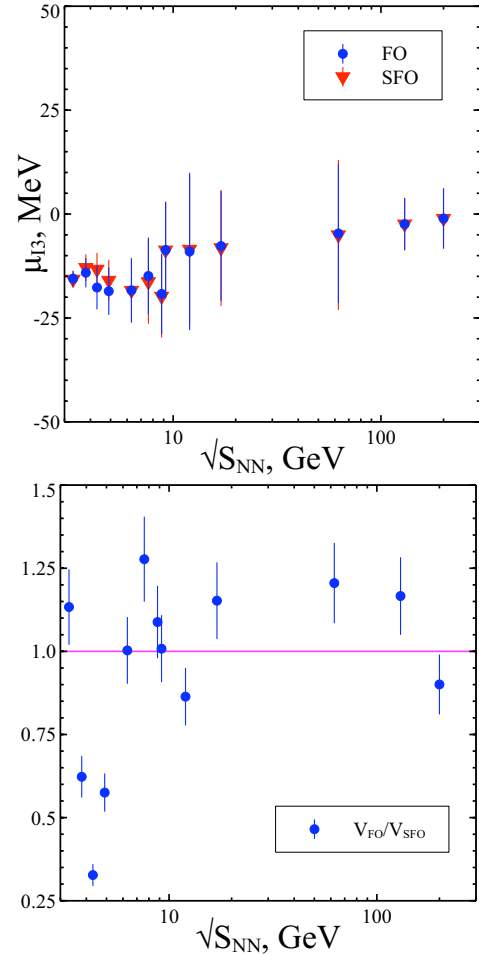


Fig. 2. Upper panel: I_3 chemical potential for the FO (circles) and the SFO (triangles) Lower panel: $\sqrt{S_{NN}}$ dependence of the ratio of the FO volume to the SFO volume.

proach compared to the case without SFO. First of all we found out that for SFO case $\chi^2/dof = 58.5/55 = 1.06$. At $\sqrt{S_{NN}} = 2.7, 3.3, 3.8, 4.3$ and 4.9 GeV the original description obtained within the multicomponent model [5] is very good and hence it has not improved significantly. Similar results are found at the highest RHIC energies $\sqrt{S_{NN}} > 62.4$ GeV. From Fig. 1 one can see that within these two energy domains the SFO temperatures demonstrate the largest deviations from the FO temperature, although they do not exceed 20%. At intermediate energies we see a systematic improvement of ratios description. Three plots corresponding to collision energies at which an improvement after SFO introduction is the most significant, $\sqrt{S_{NN}} = 6.3, 12$ and 17 GeV, are shown in Fig. 3. As one can see from Fig. 3 for $\sqrt{S_{NN}} = 6.3, 12$ and 17 GeV the SFO approach improves description of all ratios with more than one

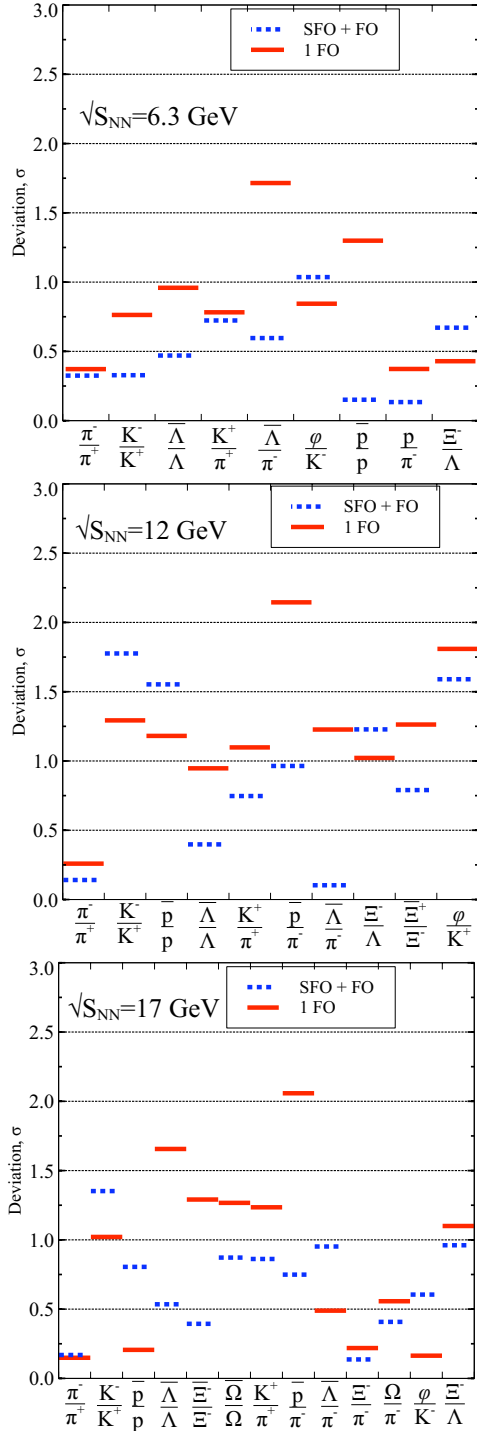


Fig. 3. Relative deviation of theoretical description of ratios from experimental value in units of experimental error σ . The symbols on OX axis demonstrate the particle ratios. OY axis shows $\frac{|r^{theor} - r^{exp}|}{\sigma^{exp}}$, i.e. the modulus of relative deviation for $\sqrt{S_{NN}} = 6.3, 12$ and 17 GeV. The solid lines correspond to a model with one chemical freeze-out of all hadrons, while the dashed lines correspond to model with the SFO.

σ deviation. For $\sqrt{S_{NN}} = 6.3$ GeV the SFO greatly improves $\bar{\Lambda}/\pi^-$ and \bar{p}/p ratios. For $\sqrt{S_{NN}} = 12$ GeV four ratios out of eight with more than one σ deviation, namely K^+/π^+ , $\bar{\Lambda}/\Lambda$, $\bar{\Lambda}/\pi^-$ and Ξ^+/Ξ^- are improved. The SFO approach allows us to significantly improve the fit quality at $\sqrt{S_{NN}} = 17$ GeV. Fig. 3 demonstrates that due to the SFO fit the six out of seven problematic ratios of the one freeze-out fit moved from the region of deviation exceeding σ to the region of deviations being smaller than σ . The most remarkable of them are \bar{p}/π^- , $\bar{\Lambda}/\Lambda$, Ξ^-/Ξ^+ and $\bar{\Omega}/\Omega$. Thus, a separation of the FO and the SFO relaxes the strong connection between the non-strange and strange baryons and allows us not only to nicely describe the ratios of strange antibaryons to the same strange baryons, but also it allows us for the first time to successfully reproduce the antiproton to pion ratio.

As we discussed above, it is expected that the SFO occurs earlier, when the system is smaller, and, hence, $V_{SFO} < V_{FO}$ or $\frac{V_{FO}}{V_{SFO}} > 1$. In the Fig. 2 one can see that this is, indeed, the case for most values of collision energy, but at low energies our expectation does not come true. One possible formal reason is the same as for an unexpected behavior of $\frac{T_{SFO}}{T_{FO}}$ (see Fig. 1): at this energy range the number of data points is just slightly larger than the number of fitting parameters and because of that at low energies of collisions the fit quality is very good without assumption of two freeze-outs. There might be also a physical reason for such a behavior, namely at low collision energies the freeze-out occurs at large baryonic densities which may essentially affect the in medium cross-sections of the reactions with strangeness exchange due to additional attraction and, therefore, such reactions do not freeze-out earlier than other reactions.

Finally, we would like to suggest a generalization of the double freeze-out HRGM that will be able to ultimately improve the description of multiplicities. The first step is to identify the hadronic reactions that freeze-out noticeably earlier or later than most of the others. This should be done separately for each collision energy, since for different energies the reaction cross-sections, the particle concentrations and the fireball expansion rate are different. Such reactions may be identified using the system (1) or by running the transport model code and counting for the reaction rates versus time. If such reactions exist, then their separate freeze-out should be considered. It is clear that the conservation laws between the freeze-outs may be different depending on what reactions are switched off. For instance, if all reactions with the Ω hyperon are frozen, then the conservation law of

the number of Ω hyperons should be introduced. Probably, the charmed particles are good candidates for the separate freeze-out.

5. Conclusions

Here we thoroughly discussed an assumption that in heavy ion collisions the strangeness exchange reactions may freeze-out earlier. Using such an assumption we constructed a modification of the HGRM with two freeze-outs, connected with the conservation laws. One freeze-out corresponds to all strange particles and another freeze-out is for all non-strange ones. The conservation laws allow us for each collision energy to get just one additional fitting parameter compared to the HRGM with a simultaneous chemical freeze-out of all hadrons. We have shown that such a model describes 111 independent hadron ratios measured at $\sqrt{S_{NN}} = 2.7 - 200$ GeV even better than the most elaborate version of the HRGM with a single freeze-out ($\chi^2/dof = 1.06$ for the model with two freeze-outs versus 1.16 for one freeze-out).

We suggest to go even further: for each collision energy to separately identify the processes which freeze-out at considerably different time than all the other and to construct a corresponding HRGM with two freeze-outs. Identification of such reactions can be done using the transport models.

Acknowledgments. The authors are thankful to P. Huovinen for fruitful discussions. D.R.O. acknowledges funding of a Helmholtz Young Investigator Group VH-NG-822 from the Helmholtz Association and GSI, and thanks HGS-HIRE for a support. A.I.I. and K.A.B. acknowledge a support of the Fundamental Research State Fund of Ukraine, Project No F58/04. Also K.A.B. acknowledges a partial support provided by the Helmholtz International Center for FAIR within the framework of the LOEWE program launched by the State of Hesse.

1. P. Braun-Munzinger, K. Redlich and J. Stachel, In **Hwa, R.C. (ed.) et al.: Quark gluon plasma**, **13**, 491 (2003).
2. A. Andronic, P. Braun-Munzinger and J. Stachel, Nucl. Phys. A **772**, 167 (2006) and references therein.
3. F. Becattini, J. Phys. G **23**, 1933 (1997).
4. F. Becattini, J. Manninen and M. Gazdzicki, Phys. Rev. C **73**, 044905 (2006).
5. K.A. Bugaev, D.R. Oliinychenko, A.S. Sorin and G.M. Zinovjev, Eur. Phys. J. A **49**, 30–1-8 (2013) and references therein.
6. B. Friman *et al.* (Eds.), *“The CBM physics book”*, Lect. Notes Phys. **814**, Springer, 2010.
7. J. Rafelski, Phys. Lett. B **62**, 333 (1991).
8. P. Braun-Munzinger, D. Magestro, K. Redlich and J. Stachel, Phys. Lett. B **518**, 41 (2001).
9. K.A. Bugaev, D.R. Oliinychenko, J. Cleymans, A.I. Ivanytskyi, I.N. Mishustin, E.G. Nikonov, V.V. Sagun, Europhys. Lett. **104**, 22002 (2013).
10. K.A. Bugaev J. Phys. G **28**, 1981 (2002).
11. M.I. Gorenstein, K.A. Bugaev and M. Gazdzicki, Phys. Rev. Lett. **88**, 132301 (2002).
12. K.A. Bugaev, M. Gazdzicki and M.I. Gorenstein, Phys. Lett. B **544**, 127 (2002).
13. E. Fermi, Prog. Theor. Phys. **5**, 570 (1950).
14. L.D. Landau, Izv. Akad. Nauk. SSSR, ser. fiz. **17**, 51 (1953).
15. J. Stachel *et al.*, arXiv:1311.4662 [nucl-th].
16. K. Redlich *et al.*, J. Phys. G. **36**, 064021 (2009).
17. M. Gyulassy and X.N. Wang, Nucl. Phys. B **420**, 583 (1994).
18. X.N. Wang, M. Gyulassy, M. Plümer, Phys. Rev. D **51**, 3436 (1995).
19. R. Baier, Yu.L. Dokshitzer, S. Peigne, D. Schiff, Phys. Lett. B **345**, 277 (1995).
20. K.A. Bugaev *et al.*, NICA White Paper, Draft 9.01, Contribution **4.21**, published on 6 of June, 2013; <http://theor.jinr.ru/twiki/pub/NICA/NICAWhitePaper>.
21. S. Chatterjee, R.M. Godbole, S. Gupta, Phys. Lett. B, **727**, 554 (2013).
22. D.R. Oliinychenko, K.A. Bugaev, A.S. Sorin, Ukr. J. Phys. **58**, 211 (2013).
23. K.A. Bugaev, M.I. Gorenstein, H. Stöcker and W. Greiner, Phys. Lett. B **485**, 121 (2000).
24. G. Zeeb, K.A. Bugaev, P.T. Reuter and H. Stöcker, Ukr. J. Phys. **53**, 279 (2008).
25. K.A. Bugaev, Nucl. Phys. A **807**, 251 (2008); arXiv:nucl-th/0611102.
26. K.A. Bugaev, D.R. Oliinychenko and A.S. Sorin, Ukr. J. Phys. **58**, 939 (2013).
27. K.A. Bugaev, A.I. Ivanytskyi, D.R. Oliinychenko, E.G. Nikonov, V.V. Sagun and G.M. Zinovjev, arXiv:1312.4367 [hep-ph].
28. K.A. Bugaev, D.R. Oliinychenko, V.V. Sagun, A.I. Ivanytskyi, J. Cleymans, E.G. Nikonov and G.M. Zinovjev, arXiv:1312.5149 [hep-ph].
29. S. Wheaton, J. Cleymans and M. Hauer, Comput. Phys. Commun. **180**, 84 (2009).
30. J.L. Klay *et al.*, Phys. Rev. C **68**, 054905 (2003).
31. L. Ahle *et al.*, Phys. Lett. B **476**, 1 (2000).

32. B.B. Back *et al.*, Phys. Rev. Lett. **86**, 1970 (2001).
33. J.L. Klay *et al.*, Phys. Rev. Lett. **88**, 102301 (2002).
34. C. Pinkenburg *et al.*, Nucl. Phys. A **698**, 495c (2002).
35. P. Chung *et al.*, Phys. Rev. Lett. **91**, 202301 (2003).
36. B.B. Back *et al.*, Phys. Rev. C **69**, 054901 (2004).
37. S. Albergo *et al.*, Phys. Rev. Lett. **88**, 062301 (2002).
38. B.B. Back *et al.*, Phys. Rev. Lett. **87**, 242301 (2001).
39. S.V. Afanasiev *et al.*, Phys. Rev. C **66**, 054902 (2002).
40. S.V. Afanasiev *et al.*, Phys. Rev. C **69**, 024902 (2004).
41. T. Anticic *et al.*, Phys. Rev. Lett. **93**, 022302 (2004).
42. S.V. Afanasiev *et al.*, Phys. Lett. B **538**, 275 (2002).
43. C. Alt *et al.*, Phys. Rev. Lett. **94**, 192301 (2005).
44. S.V. Afanasiev *et al.*, Phys. Lett. B **491**, 59 (2000).
45. B. Abelev *et al.*, Phys. Rev. C **81**, 024911 (2010).
46. B. Abelev *et al.*, Phys. Rev. C **79**, 034909 (2009).
47. J. Adams *et al.*, Phys. Rev. Lett. **92**, 182301 (2004).
48. J. Adams *et al.*, Phys. Lett. B **567**, 167 (2003).
49. C. Adler *et al.*, Phys. Rev. C **65**, 041901(R) (2002).
50. J. Adams *et al.*, Phys. Rev. Lett. **92**, 112301 (2004).
51. J. Adams *et al.*, Phys. Lett. B **612**, (2005) 181.
52. A. Billmeier *et al.*, J. Phys. G **30**, S363 (2004).